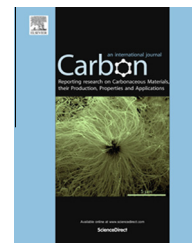


Available at www.sciencedirect.com

ScienceDirect

journal homepage: www.elsevier.com/locate/carbon

Unravelling the roles of surface chemical composition and geometry for the graphene–metal interaction through C1s core-level spectroscopy

Francesco Presel ^a, Naila Jabeen ^{a,b,c}, Monica Pozzo ^d, Davide Curcio ^a, Luca Omiciuolo ^a, Paolo Lacovig ^e, Silvano Lizzit ^e, Dario Alfè ^{d,f}, Alessandro Baraldi ^{a,e,g,*}

^a Physics Department, University of Trieste, Via Valerio 2, 34127 Trieste, Italy

^b International Centre for Theoretical Physics, Strada Costiera 11, 34151 Trieste, Italy

^c Nanosciences & Catalysis Division, National Centre for Physics, Islamabad 44000, Pakistan

^d Department of Earth Sciences, Thomas Young Centre@UCL, London Centre for Nanotechnology, University College London, Gower street, London WC1E 6BT, United Kingdom

^e Elettra – Sincrotrone Trieste S.C.p.A., AREA Science Park, S.S. 14 km 163.5, 34149 Trieste, Italy

^f IOM-CNR, DEMOCRITOS National Simulation Centre c/o SISSA, Via Bonomea 265, 34136 Trieste, Italy

^g IOM-CNR, Laboratorio TASC, AREA Science Park, S.S. 14 km 163.5, 34149 Trieste, Italy

ARTICLE INFO

Article history:

Received 25 March 2015

Accepted 10 May 2015

Available online 21 May 2015

ABSTRACT

Here we show that by using a combined experimental and theoretical approach it is possible to separate the contributions to the interaction strength between epitaxial graphene and transition metal surfaces arising from the geometrical and chemical properties of the supporting surfaces. This has been achieved by performing photoelectron measurements and numerical simulations of the C1s core level spectral distribution for a large number of graphene–metal systems, which have been obtained by systematic intercalation of different metals (Co, Rh, Ir and Ru) at the graphene–Ir(111) and graphene–Ru(0001) interfaces. We demonstrate that the chemical species of the substrate's topmost layer plays a major role in determining the coupling between graphene and its substrate. Moreover, we show that both the experimental and the theoretical C1s spectral centres of mass are in linear relationship with the d-band centre of the transition metal substrate, which is considered a reliable descriptor of the graphene–substrate interaction strength. Our results provide a simple method to determine and tailor the properties of graphene–metal contacts.

© 2015 Elsevier Ltd. All rights reserved.

1. Introduction

The unique band structure and a high mobility and density of charge carriers are just some of the remarkable properties of graphene [1,2] which make it one of the most studied materials

for the development of innovative nanoelectronic devices [3]. The synthesis of graphene on a metal surface by means of Chemical Vapour Deposition (CVD) is a technique which allows to obtain high quality graphene monolayers with a low density of defects [4] and ensures an efficient electric contact with a

* Corresponding author at: Physics Department, University of Trieste, Via Valerio 2, 34127 Trieste, Italy.
E-mail address: alessandro.baraldi@elettra.eu (A. Baraldi).

<http://dx.doi.org/10.1016/j.carbon.2015.05.041>

0008-6223/© 2015 Elsevier Ltd. All rights reserved.

conducting surface, which is instead not trivial to establish at a later stage [5]. The interaction of graphene with metal surfaces, however, causes modifications to those properties that make it unique, mainly because of charge transfer processes, re-hybridization and changes to its band structure [6–8]. Moreover, magnetic substrates can induce magnetization of the graphene lying on top, as has been demonstrated for graphene on Ni(111) [9], and this could be used for interesting applications of graphene such as magnetic tunnel junctions and innovative memory devices [10,11]. A good understanding of the interactions occurring at interfaces between graphene and metals is therefore required to create high-performance graphene-based nanoelectronic devices [6].

Metallic surfaces where graphene can be grown or deposited can be classified depending on the degree of interaction they establish with it [12,13]. Some show a weak, van der Waals-like coupling and are characterized by a graphene–surface separation close to the interlayer distance of graphite (around 3 Å), such as Ir(111) [14] and Pt(111) [15]. Others, instead, display a much stronger interaction, such as Ru(0001) [16–18] and Re(0001) [19,20]: in these cases, the graphene–surface distance is reduced, the nearest carbon atoms lying at approximately 2 Å from the metallic surface. Buckling of the graphene layer is often present. Moreover, the band structure of graphene is strongly modified, with the disappearance of the Dirac cones and the opening of a band gap at the Fermi level [21].

The alterations to the electronic structure in the former case can be explained in terms of a difference in the work functions of graphene and the metal substrate, which induces a charge transfer at the interface and a shift of the Fermi level, resulting in the formation of a surface dipole moment [6]. For strongly interacting systems, however, there is still debate as to what determines the interaction strength between graphene and its metal substrate [13,21].

One possibility is related to the mismatch between the lattice parameter of graphene and that of the underlying surface which induces a different degree of re-hybridization on different C atoms, and is known to drive the formation of moiré superstructures of epitaxial graphene on transition metals [22]. The geometry of the metallic surface not only causes strain on graphene as its lattice parameter adapts to that of the substrate, but could also influence its electronic properties. It has been demonstrated, in fact, that graphene on Cu has a different degree of doping depending on the symmetry of the surface over which it has been grown: (111), (110) or (100) [23].

On the other hand, one can quantify the interaction by extending Hammer and Nørskov's model for the chemisorption of molecules on transition and noble metal surfaces [24] also to graphene/metal systems [16,25]. This model explains the chemical bonding between molecules and surfaces with a coupling between the valence orbitals of the adsorbates and the metal d-bands. This coupling is maximum when the orbitals of the molecule lie close in energy to the metal d-band centre. In fact it has been shown that all surfaces which exhibit the strongest interaction with graphene have a d-band centre lying around 1 eV below the Fermi level,

whereas the interaction weakens as the barycentre moves further away from it [13]. Also the spin polarization of graphene on magnetic surfaces such as Ni(111) can be described in terms of the hybridization between the metal's d-band and graphene's π states [9]. The differences in the interaction energy of graphene with transition metal surfaces have been actually measured employing a nanoscale mechanical exfoliation technique based on nano-scratching of graphene [26].

In order to understand the changes in graphene's electronic structure induced by the coupling with different substrates, angular resolved photoemission spectroscopy (ARPES) is very often applied [7,15,27–33], as well as X-ray absorption (XAFS), Raman and electron energy loss spectroscopies [8,27,34]. However, one of the limits of these powerful approaches is that they do not allow to distinguish carbon atoms in non-equivalent local configurations of the moiré structures which are typically formed by graphene on top of the metal surfaces. High energy resolution measurements of the C1s core level, on the other hand, allow to study the electronic structure of metal-supported graphene layers in great detail [12], since the dispersion of this level, which has actually been observed despite its being a core level, is very small [35]. High energy resolution core level spectroscopy has proved particularly effective in determining the doping of weakly interacting graphene and in demonstrating its relationship with the work function of surfaces, since the energy shift of the core levels reflects that of the valence band [36]. In the case of strongly interacting graphene, however, chemical bonding between the substrate and graphene introduces a chemical shift in the core levels and the Binding Energy (BE) does not depend exclusively on doping any more.

The primary aim of our combined experimental and theoretical investigation is then to distinguish the contributions arising from the geometrical (lattice mismatch) and chemical (elemental composition of the substrate) properties of the surface on the interaction between graphene and metals, and to verify whether C1s core level shifts are directly linked to the surface chemical reactivity of the supporting metal substrates.

We have achieved this by systematic intercalation of different metallic species at graphene–metal interfaces, following the scheme reported in Fig. 1, a method which has proved effective in decoupling graphene from the strongly interacting Ni(111) surface [34]. The intercalation process, in fact, modifies the chemical composition of the first surface layer while preserving the symmetry and the lattice constant of the substrate, provided the intercalated layer is of monatomic thickness. In order to make an extensive comparison in controlled and reproducible conditions on model systems, different single-crystal close-packed metallic surfaces were used, one which interacts strongly with graphene (Ru(0001), $l_{\text{Ru}} = 2.70$ Å) and one which interacts weakly with it (Ir(111), $l_{\text{Ir}} = 2.72$ Å). Both substrates have a lattice parameter which is larger than that of graphene ($l_{\text{GR}} = 2.46$ Å). The intercalated species were also chosen in such a way that each of them possesses a different degree of interaction with graphene when the latter is grown on their hexagonal close-packed surface: besides Ru and Ir, we employed Rh (which exhibits an

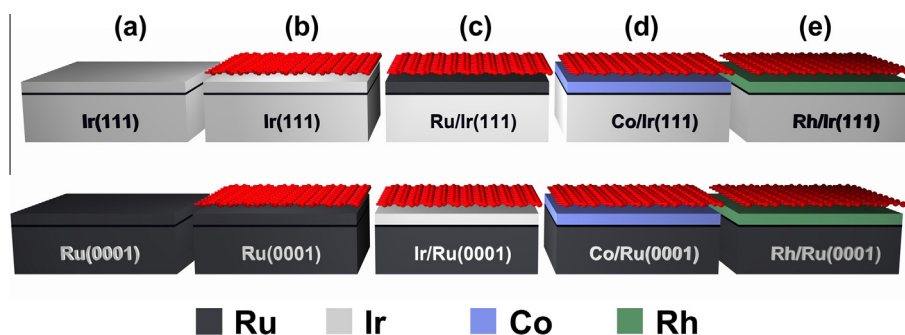


Fig. 1 – Schematic outline of the experimental procedure followed in the present work. (a) Pristine monocrystalline Ir(111) (top row) and Ru(0001) (bottom row) surfaces. (b) Graphene growth. (c–e) Intercalation of different metallic species at the graphene/metal interface. (A colour version of this figure can be viewed online.)

intermediate interaction strength with graphene) and Co (which is even more strongly interacting than Ru).

2. Methods

2.1. Experimental

All experiments were performed in Ultra High Vacuum conditions, with base pressure never exceeding 2×10^{-10} mbar, at the SuperESCA beamline [37] and at the Surface Science Laboratory of the Elettra synchrotron radiation facility. All photoemission spectra were measured at the beamline in normal emission conditions; the electron BE scale was calibrated using the Fermi edge measurement in the same conditions. The C1s spectra were measured using a photon energy of 385 eV with an overall experimental resolution of 40 meV. Graphene was grown on Ir(111) and Ru(0001) surfaces using well established procedures [18,38,39]. Its quality was verified by measuring in situ the C1s core level spectra and the Low Energy Electron Diffraction (LEED) pattern (further details are provided in [supporting information](#)).

The intercalation of each metal was obtained by evaporation while keeping the sample surface at 700 K. This temperature was chosen because it generally allows metal atoms to have enough mobility to diffuse above graphene, reach a suitable site for intercalation (mainly grain boundaries) and diffuse below the surface, while it has been demonstrated that metallic species deposited at ambient temperature usually tend to form clusters on top of graphene, without intercalating [40–43]. After each deposition, we verified that the deposited metals had indeed intercalated by monitoring the Ir $4f_{7/2}$ or Ru $3d_{5/2}$ core levels' line-shape (see [supporting material](#)). LEED measurements confirmed that the lattice parameters were not modified by the intercalation, i.e. the intercalated layer was pseudomorphic.

About 1 monolayer (ML) of metal was deposited for each system, in steps of approximately 0.1 ML each. The evolution of the chemical, structural and electronic properties was followed by acquiring the core-level spectra of graphene (C1s). The photoemission spectra of the metallic substrate (either Ir $4f_{7/2}$ or Ru $3d_{5/2}$) and of the intercalated species (Ir $4f_{7/2}$, Ru $3d_{5/2}$, Co $3p_{3/2}$ and Rh $3d_{5/2}$) were also acquired: the analysis of these latter peak intensities was used to determine the coverage of the intercalated metals (see [supporting information](#)).

After each intercalation step, the surface was cleaned by means of repeated cycles of sputtering and annealing. The surface cleanliness was again verified through photoemission measurements before regrowing graphene using the same procedures.

All photoemission spectra were fitted to a sum of Donjachić–Šunjić (DS) lineshapes [44] — characterized by a Lorentzian width Γ , which takes into account the effect of finite core-hole lifetime, and by the asymmetry index α , which describes the low-energy electron–hole pair excitations near the Fermi level — convoluted with a Gaussian distribution (full width at half-maximum G) — which takes into account phonon, inhomogeneous and instrumental broadening. The inelastic contribution was modelled using a Shirley background [45,46].

2.2. Theoretical

Calculations were performed using Density Functional Theory [47,48] with exchange–correlation effects included at the level of the PBE-GGA [49] functional. We used the Projector Augmented Wave [50] (PAW) method as implemented in VASP [51,52] to account for the core electrons of both metals and C atoms, with the 6s and 5d electrons of Ir, 5s and 4d electrons of Rh and Ru, 4s and 3d electrons of Co and the 2s and 2p electrons of C explicitly included in the valence. We used a plane-wave kinetic energy cut-off of 400 eV.

The structures were obtained by overlaying a graphene sheet over a (12×12) and a (9×9) supercell for Ru(0001) and Ir(111) respectively, using a $3 \times 3 \times 1$ grid to sample the surface Brillouin zone. The metal surfaces were modelled using a slab with a thickness of 5 layers, with the atoms of the 2 bottom layers kept fixed at their bulk positions, while all the other atoms were allowed to relax. By modifying the chemical species of the topmost metallic layer we were also able to model the systems obtained from the intercalation of metals below graphene. A vacuum interspace of at least 15 Å (between metallic layers, excluding graphene) was used to minimize the interaction between periodic images of the slab along the direction perpendicular to the surface, resulting in a super-cell of 24 Å along the z axis.

This approach allows to describe systems where a single layer of metal is intercalated below graphene with high accuracy; however, it does not take into account local defects,

which are inevitably present in real systems, such as vacancies or 3-dimensional islands composed of two (or more) layers of intercalated metal.

Core-level BEs for C atoms have been estimated in the so-called final-state approximation. This estimate does not include the effect of core electron screening, as the other core electrons remain fixed at the electronic configurations used to generate the PAW potential. However the screening from valence electrons is included, thus providing an accurate estimate of its effect on the core level BE. Although the core level energies themselves are not directly accessible because of the frozen core approximation, differences of core level energies are accurately reproduced [53].

The positions of the d-band centre E_d with respect to the Fermi energy E_F for the different graphene-free metal surfaces has been calculated as

$$E_d = \int_{-\infty}^{E_0} dE(E - E_F)pd(E)$$

where $pd(E)$ is the electronic density of states obtained by projecting the Kohn–Sham orbitals onto spherical harmonics of type d centred on the metal atoms, and E_0 is a cut-off energy that we chose to be 7 eV above the Fermi energy.

3. Results and discussion

3.1. Experimental results

All photoemission components of the C1s core level which appear in any of the systems we analysed are reported in Table 1, together with their BEs. The analysis of the C1s spectra of graphene on Ru(0001) (Fig. 2a) was complicated by the overlap of the 1s core level of carbon and the $3d_{3/2}$ core level of Ru. It was therefore necessary, in the analysis of the C1s spectrum, to include the Ru $3d_{3/2}$ core level, determining its lineshape from the $3d_{5/2}$ component (see supplementary material). The same procedure has been adopted for the analysis of all spectra acquired during the intercalation of each metal on the Ru(0001) surface, as well as for the intercalation of Ru on Ir(111).

The C1s spectrum of epitaxial graphene on Ru(0001) (Fig. 2a) shows two distinct components, a weaker one (S3) at 284.47 eV and a more intense and narrower one (S1) at 285.13 eV. The presence of two components is widely recognized as a sign of the corrugation of graphene on Ru(0001) [12,16–18]. They arise from a continuous distribution of non-

equivalent atomic configurations where the component at lower BE is mainly generated by the atoms in the higher portion of the corrugation, and the one at higher BE is generated by atoms closer to the substrate, thus showing a more pronounced interaction with the metal underneath [12,18,54]. In contrast, the C1s spectrum of graphene grown on Ir(111) (shown in Fig. 3a) is dominated by a single very narrow component (W) at a BE of 284.12 eV, which is a fingerprint of quasi free-standing graphene on Ir(111) [12,55].

In the series of spectra acquired during each intercalation experiment, it is clear that the C1s spectrum (Figs. 2b–d and 3b–d) changes dramatically as the substrate is covered by the intercalated species. In order to accurately analyse the data, we first obtained the lineshape parameters (Γ , α , G) from the spectra acquired at the highest coverage of the intercalated species, and assumed that the lineshape of each component (Γ , α) was constant throughout all the experiment, whereas the Gaussian parameter G was allowed to change, in order to describe possible contributions due to structural inhomogeneities.

For all of the graphene/metal/Ir(111) systems (Fig. 3b–d) we observe that the W component loses intensity upon intercalation, almost completely vanishing for the highest coverage. On the other hand, several components appear at a higher BE, indicating a stronger degree of interaction between graphene and the substrate. The BE of these components does not depend on the coverage, only the relative intensities being modified throughout the experiment.

Specifically, after Rh intercalation (Fig. 3b) we see a main component at 284.42 eV (S3) and two additional components, with lower intensities, at higher BEs (S1–2) (Table 1). It can be noticed that the BE of the S3 peak is quite similar for this system and for the low BE component of graphene grown on Rh(111), thus suggesting that this component could arise from buckled areas of the graphene sheet. Component S1, on the other hand, is close in BE to the high BE component of graphene on Rh(111), and is most likely related to carbon atoms strongly interacting with the substrate [56–58]. Component S2, lying in between, most probably arises from atoms in an intermediate configuration between the two.

A similar behaviour is observed for the intercalation of Ru on Ir(111) (Fig. 3c): also in this case, three components (S1–3) are detected (Table 1), lying between 284.41 and 285.10 eV. These components have BEs close to those found for the Rh intercalation. Their relative intensities, however, are different from the previous case, as the component at higher BE (S1)

Table 1 – BE of each component of the C1s core level photoemission spectrum in all systems studied in this work. The main component in the spectrum of each system is indicated in bold.

System	S1 (eV)	S2 (eV)	S3 (eV)	W (eV)
GR/Ru(0001)	285.13 eV	–	284.47 eV	–
GR/Ir/Ru(0001)	–	284.89 eV	–	284.23 eV
GR/Rh/Ru(0001)	285.13 eV	284.91 eV	284.47 eV	–
GR/Co/Ru(0001)	–	284.97 eV	284.47 eV	–
GR/Ir(111)	–	–	–	284.12 eV
GR/Rh/Ir(111)	285.05 eV	284.83 eV	284.42 eV	–
GR/Ru/Ir(111)	285.10 eV	284.75 eV	284.41 eV	–
GR/Co/Ir(111)	–	284.93 eV	284.40 eV	–

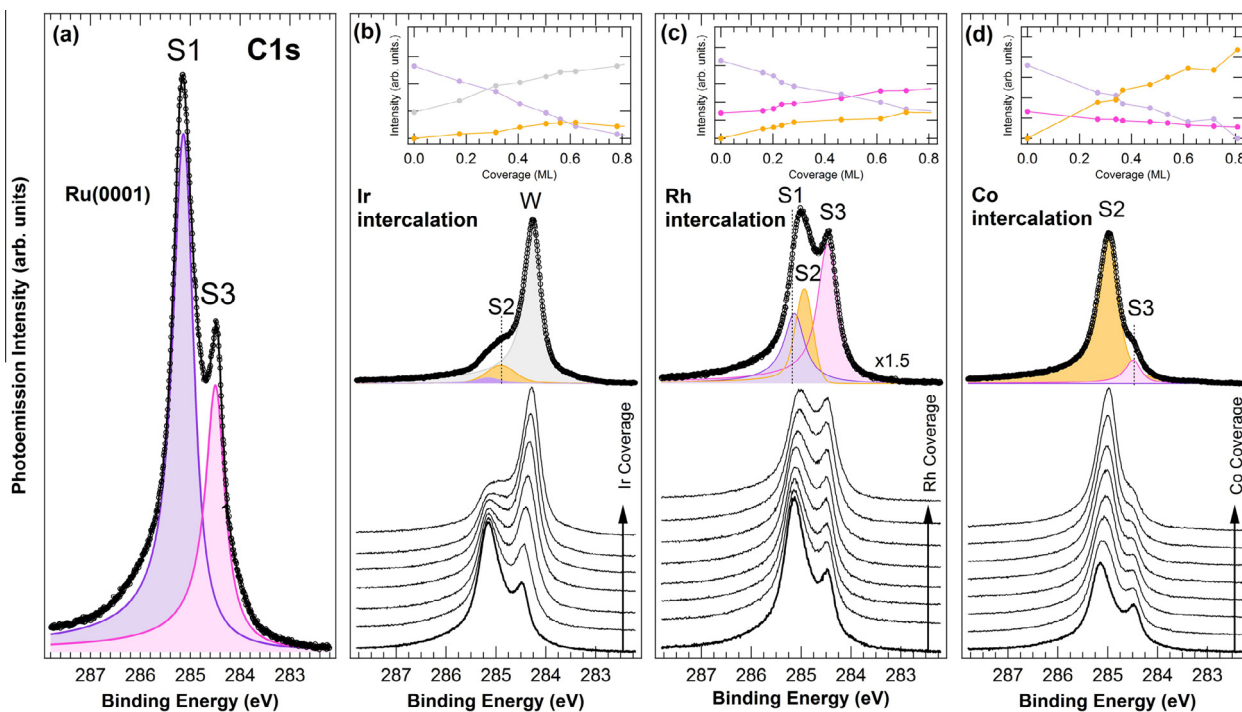


Fig. 2 – Background subtracted C1s core level spectra of graphene/Ru(0001) during intercalation ($h\nu = 385$ eV). (a) Graphene/Ru(0001), with components S1 and S3 corresponding to strongly and weakly interacting carbon atoms respectively. (b–d) Evolution of the C1s spectrum during intercalation of (b) Ir, (c) Rh and (d) Co. Top graphs show the evolution of the area of all C1s photoemission components corresponding to non-equivalent C populations at increasing intercalating metal coverages. (A colour version of this figure can be viewed online.)

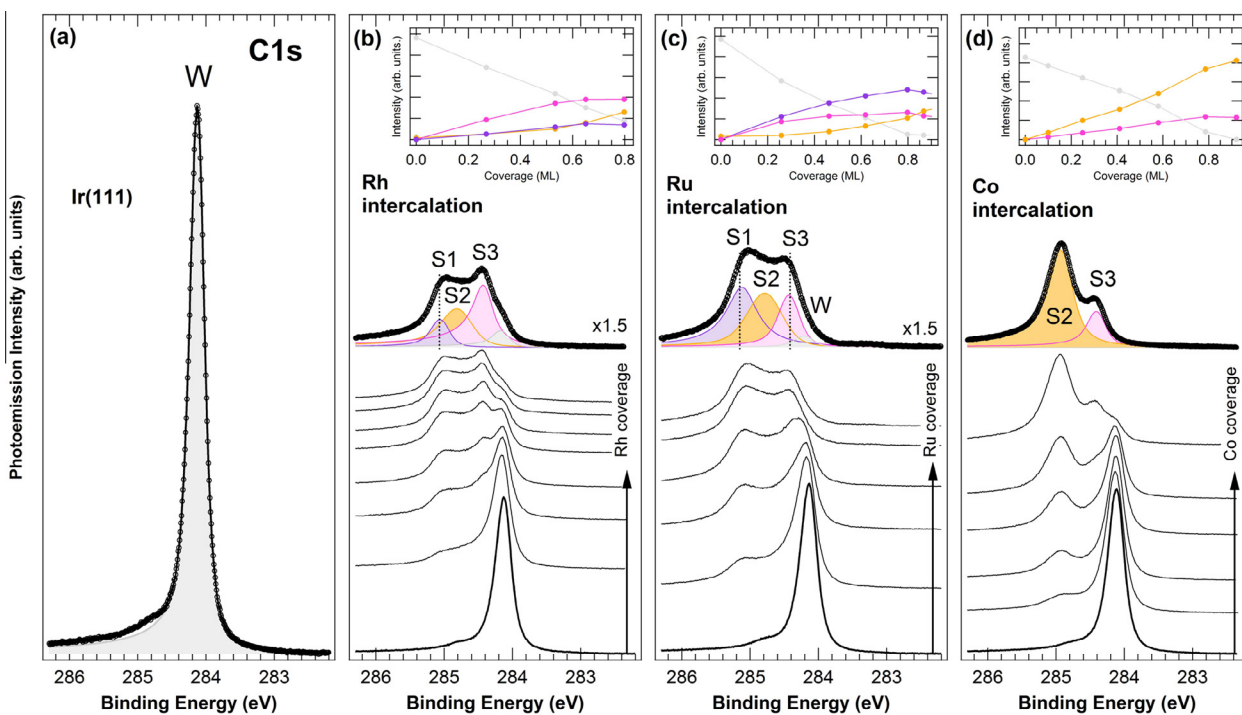


Fig. 3 – C1s core level spectra of graphene/Ir(111) during intercalation ($h\nu = 385$ eV). (a) Graphene/Ir(111), showing a single component (W). (b–d) Evolution of the C1s spectrum during intercalation of (b) Rh, (c) Ru and (d) Co. Top graphs show the evolution of the area of all C1s photoemission components corresponding to non-equivalent C populations at increasing intercalating metal coverages. (A colour version of this figure can be viewed online.)

has a larger (almost double) spectral weight than the low BE one (S3): this could indicate, on average, a stronger interaction with the Ru layer than for the Rh layer. Besides the presence of the S2 component, the spectral distribution is quite similar to the one of graphene directly grown on Ru(0001) (Fig. 2a).

Finally, for the Co evaporation on Ir(111), we obtained a large component (S2) at 284.93 eV, and a weaker one (S3) at lower BE (Table 1), indicating a generally strong interaction with the Co layer.

By comparing the intercalation experiments on Ir(111), we notice that the C1s core electrons of graphene (and therefore also its interaction with the substrate) show significant changes depending on the chemistry of the substrate. In particular, the interaction increases when passing from Ir to Rh, Ru and finally Co, which has, on average, the strongest interaction with graphene among the systems studied.

Also for the experiments performed on Ru(0001) we observe a very different behaviour depending on the element being intercalated. In the case of Ir intercalation (Fig. 2b) we notice a weakening of component S1, which almost completely disappears, while another weak component is present at lower BE (S2). The intensity of component S3, however, increases until it becomes dominant, while its BE moves linearly towards lower values, reaching 284.23 eV at a coverage of 0.8 ML (Table 1). At this point, the spectrum strongly resembles that of graphene grown on Ir(111) and the dominant component is similar to component W of the latter system. This change in BE can be attributed to a smooth modification of the properties of graphene, from few-atom buckling above Ru(0001) towards a completely raised, weakly interacting graphene above the Ir layer. The presence of the weak component S2 could be attributed to the formation of local defects and to inhomogeneities in the distribution of the Ir atoms.

Also the intercalation of Rh on Ru(0001) (Fig. 2c) leads to an increase in the low BE component (S3). In addition, there are two weaker components (S1–2) at higher BE (Table 1). In this case, though, there are no changes in the BE of any component, indicating that the modifications are limited to a change in populations of weakly and strongly interacting atoms.

Finally, after the intercalation of Co on Ru(0001) (Fig. 2d) the high BE component (S1) is replaced by a new one (S2), at a slightly lower BE (Table 1). These two components are always distinct and their BEs remain constant with increasing Co coverage. On the other hand, the low-BE component (S3) decreases: in general the spectral weight moves towards higher BE, indicating a slightly stronger interaction of graphene with Co than with Ru.

In conclusion, we observe a very similar trend to the experiments on Ir(111), in which the spectrum greatly varies depending on the chemical composition of the topmost layer of the substrate, with which graphene interacts. Also in this case, we found that the interaction with Ir is the weakest, followed by Rh and Ru. Only Co has an interaction with graphene stronger than Ru.

3.2. Theoretical results

Figs. 4 (intercalated layer on graphene/Ru(0001)) and 5 (intercalated layer on graphene/Ir(111)) show the theoretically

simulated minimum-energy geometric configuration for all the systems studied in this experiment. The colour scale indicates the vertical distance (z) of each carbon atom from the surface plane of the metallic substrate. The metallic substrate itself is actually corrugated when it strongly interacts with graphene. This corrugation, however, is an order of magnitude lower than that of graphene. For this reason, the vertical distance has been referred to the mean vertical position of all atoms composing the metallic surface.

For all systems, graphene's properties strongly depend on the chemical composition of the topmost layer of the substrate. In particular, where the topmost layer consists of Ir (Figs. 4a and 5a), the distance between graphene and the substrate is larger than 4 Å and the former has a very small corrugation. This is in contrast with all other systems, where the distribution is much wider, with the nearest atoms closer than 2 Å to the surface and the farthest between 3.4 and 3.9 Å. For all systems, the unit cells of graphene whose atoms are farthest from the surface are those where the centre of the honeycomb lies in an on-top site of the substrate, and therefore both atoms lie in hollow sites. On the other hand, the cells closest to the substrate are those where the centre of the honeycomb lies in bridge sites, and both C atoms lie above a metallic atom.

In particular, the distribution along z of the atoms of graphene above a Co layer (Figs. 4d and 5d) has a very sharp peak at low z values (between 1.9 and 2.1 Å), with only a small number of atoms located at more than 2.1 Å from the surface (and up to 3.5 Å), 25% of all C atoms on Ir(111) and 13% on Ru(0001).

In the case of graphene on Ru, most of the C atoms lie at a small distance from the substrate (between 2.1 and 2.3 Å). The others, which are more than 25% in the case of graphene/Ru(0001) and almost 50% for graphene/Ru/Ir(111), lie at a higher distance, reaching up to 3.7 Å on the former substrate (Fig. 4c) and up to 3.9 Å above the latter (Fig. 5c). The number of weakly interacting C atoms and the range of the C atoms' z values for Ru are larger than for Co, indicating a slightly weaker average interaction.

Finally, the distance of graphene from the Rh layer has a quite uniform distribution which ranges from 2.1 to 3.7 Å for Ru(0001) (Fig. 4b), and from 2.1 to 3.9 Å for Ir(111) (Fig. 5b), thus suggesting a smoother corrugation and a weaker interaction of graphene with Rh than with Co or Ru, but still stronger than with Ir.

The calculated distance between graphene and Ru(0001) is in good agreement with experimental values found in literature [59]. This is also the case of the separation between graphene and intercalated Co on Ir(111), which is in very good agreement with previous experiments on the same system [60]. Moreover, the z value of about 2 Å found for the majority of atoms in both systems corresponds to the height found for all atoms of graphene above Co(0001), where graphene matches the lattice of the surface forming a 1×1 commensurate structure [13,61]. The two systems where graphene lies above an intercalated Rh layer have the same corrugation as graphene on Rh(111) [13,62]. The separation of graphene from Ir(111) appears instead to be overestimated, being by more than 1 Å larger than the inter-layer distance of graphite [14].

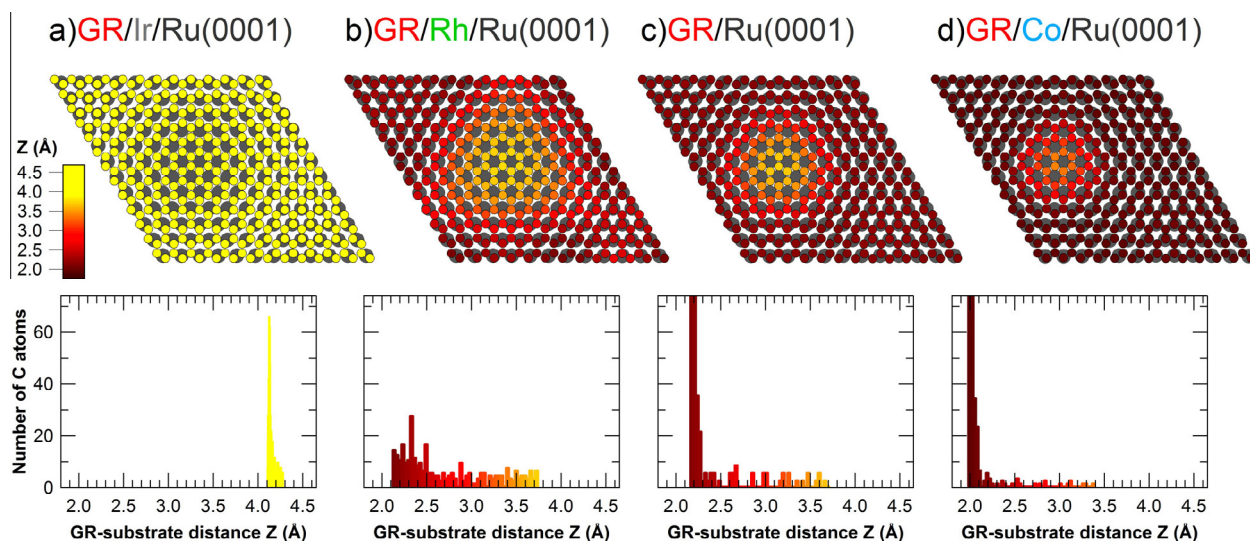


Fig. 4 – Theoretical results for different graphene/metal/Ru(0001) interfaces. Top panels: geometric configuration of the topmost metallic atoms (large, gray circles) and of the carbon atoms (smaller, coloured circles) inside the (13×13) moiré unit cell. The C atom colour scale indicates the C to substrate distance z . Bottom panels: distribution of all C-metal substrate distance z in the moiré unit cell. (A colour version of this figure can be viewed online.)

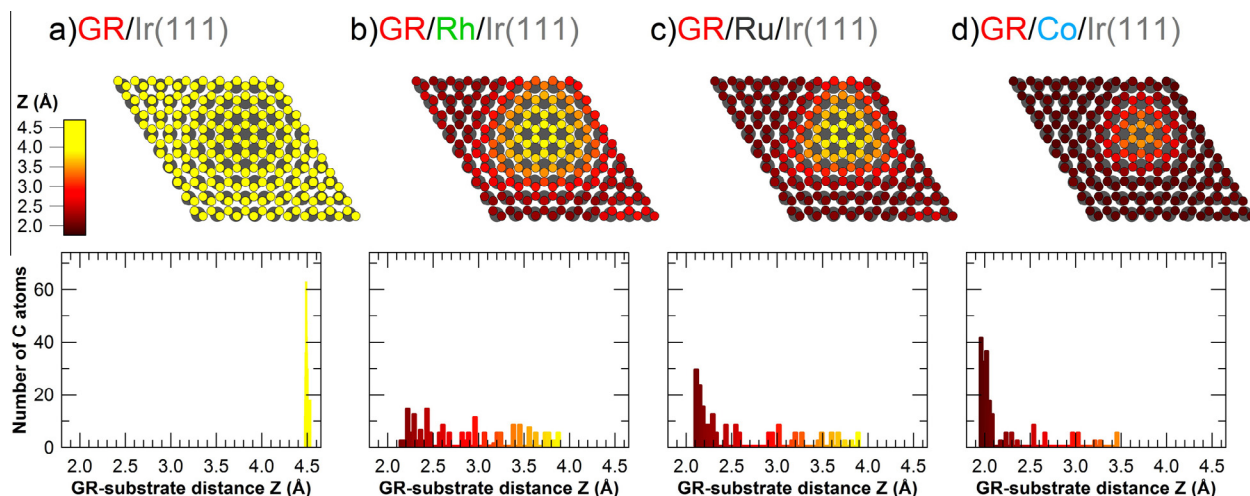


Fig. 5 – Theoretical results for different graphene/metal/Ir(111) interfaces. Top panels: geometric configuration of the topmost metallic atoms (large, gray circles) and of the graphene atoms (smaller, coloured circles) inside the (9×9) moiré unit cell. The C atom colour scale indicates the C to substrate distance z . Bottom panels: distribution of all C-metal substrate distance z in the moiré unit cell. (A colour version of this figure can be viewed online.)

This can be attributed to the presence of dispersive forces which are not included in the present calculations [25,63] and which are not negligible in this case.

The DFT calculations were also used to calculate the core level BEs of all C atoms, but since such theoretical methods only provide the relative positions of the C1s BEs for non equivalent atoms, we first had to rigidly shift the energy scale to align its reference to that of the measured data. To this purpose we first aligned the centre of the calculated BE distribution for the Ir(111) system to the actual experimental data, and then shifted the BE scale for all systems by the same offset. The graphene/Ir(111) system was chosen because it displayed both the narrowest experimental spectrum and

theoretical BE distribution, thus minimizing the error in the calibration.

The 1s BE distributions of the C atoms inside the moiré cell for each of our systems are reported in Figs. 6 and 7. A different behaviour of the C1s BEs distribution can be observed for different chemical compositions of the substrate's topmost layer, regardless of its geometry. Graphene lying above Ir has a very narrow distribution of C1s BEs, centred around 284.20 eV for graphene on Ir(111) (Fig. 7a), and between 284.25 and 284.28 eV for graphene on Ir intercalated on Ru(0001) (Fig. 6a). On the other hand, the distribution is much wider for graphene sitting on Rh, Ru and Co (Figs. 6b-d and 7b-d). Most of the computed C1s BEs, in fact, fall in the range

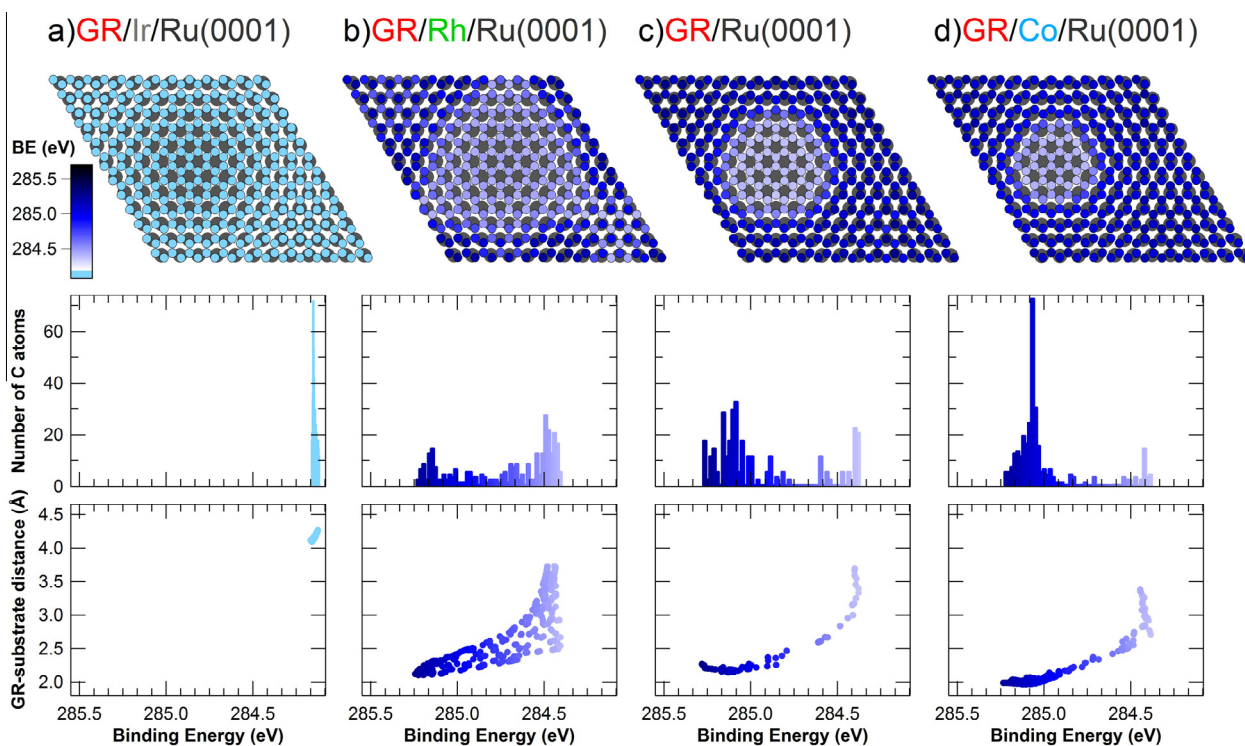


Fig. 6 – Theoretical results for graphene/metal/Ru(0001) systems. Top panels: the C1s core level BE is represented for each C atom (small dots) in the moiré cell using a colour scale. The larger, gray circles represent the underlying metallic atoms. Middle panels: Distribution for BEs of all C atoms. Bottom panels: correlation between C1s BE and separation of each atom from the topmost metallic layer. (A colour version of this figure can be viewed online.)

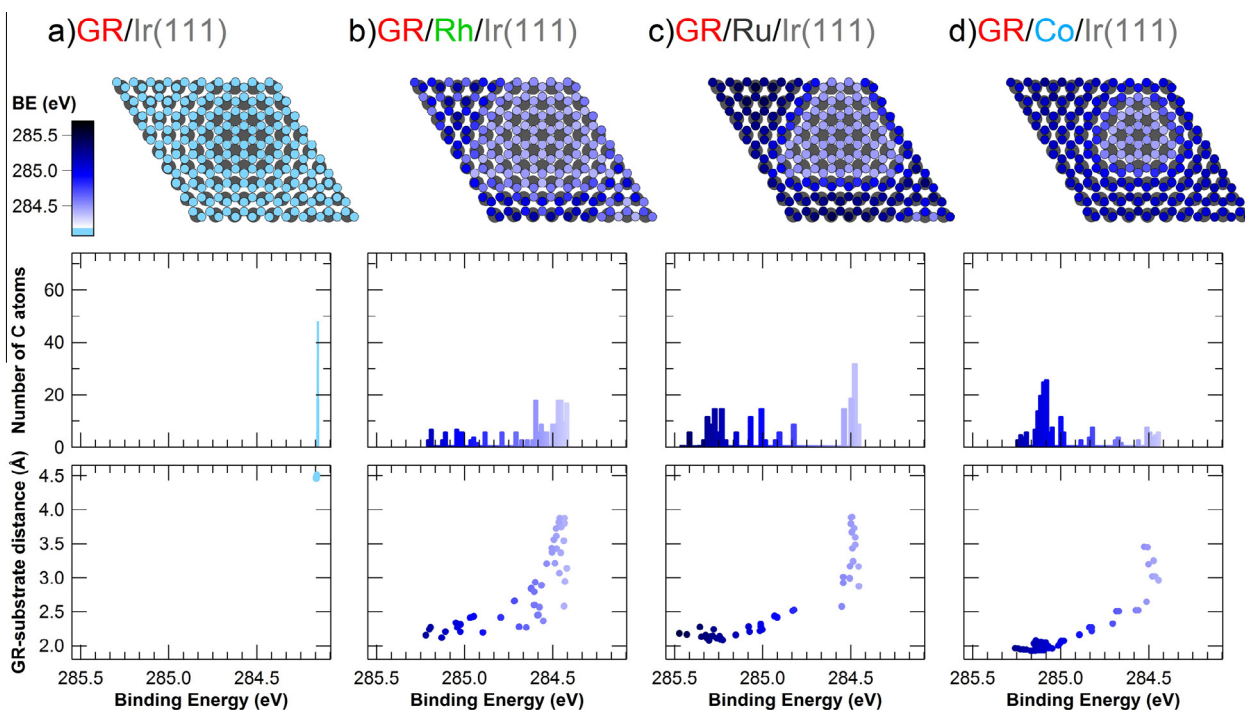


Fig. 7 – Theoretical results for graphene/metal/Ir(111) systems. Top panels: the C1s core level BE is represented for each C atom (small dots) in the moiré cell using a colour scale. The larger, gray circles represent the underlying metallic atoms. Middle panels: Distribution of BEs for all C atoms. Bottom panels: correlation between C1s BE and separation of each atom from the topmost metallic layer. (A colour version of this figure can be viewed online.)

between 284.50 and 285.35 eV and in some systems — such as Ru on Ir(111) (Fig. 7c) — can reach up to 285.5 eV. What differs among these corrugated systems, however, is the shape of the distribution, which is different depending on the topmost metallic layer. Around 50% of the C atoms lying above Rh have closely spaced C1s BEs ranging between 284.5 and 284.7 eV, while the others are evenly distributed at higher BEs. On the other hand, most atoms of graphene above Ru have a C1s BE between 285.1 and 285.3 eV, while only around 13% of the atoms above Ru(0001) and 25% of those above Ru on Ir(111) are concentrated at low BE. Finally, C atoms belonging to graphene lying above Co have a sharp peak in their C1s BE distribution centred at around 285.20 eV, with only around 15% of the C atoms having a 1s BE lower than 284.7 eV.

As can be observed in the bottom graphs in Figs. 6 and 7, there is usually a correlation between the distance of each carbon atom from the underlying surface and its C1s BE, with the latter decreasing as the former increases. The situation is more complicated for the case of graphene on Rh (Fig. 6b), where some adjacent atoms, despite being at the same distance from the substrate (about 2.5 Å), show a large difference (up to 500 meV) in the C1s BE. In this case, in fact, the energy of each atom is related to the site it occupies on the surface: in particular, the BE is maximum for atoms occupying on-top or bridge sites and minimum for threefold hollow sites. This particular behaviour has already been observed for epitaxial graphene on Rh(111) and has been explained in terms of the hybridization of the π states of graphene not only with the d_{z^2} but also with the d_{zx} and d_{zy} bands of Rh [64]. This dependence of the BE on the site is not observed for atoms either too close to the surface (around 2 Å) or too far (above 3 Å).

The theoretical simulations also allowed us to compute the average distance of each C atom from its three nearest neighbours; the distribution is described in detail in the supporting information. This is one of the parameters influenced by geometry: since the moiré unit cell is preserved in the intercalation process, the average separation between C atoms is larger (by around 0.02 Å) in systems having the moiré unit cell of graphene/Ru(0001) than in systems having the moiré unit cell of graphene/Ir(111).

The similarity between the histograms representing the C1s BE distribution and the measured XPS spectra for each of the systems studied in this work underlines the accuracy and validity of the calculations. In order to further confirm their agreement, we have compared the barycentre of each calculated distribution with that of the corresponding experimental spectrum. To do this with the best possible accuracy, we calculated it for all the coverages up to a monolayer, and then used the value obtained through a linear fit. In most systems, the experimental values agree with the calculated ones, within an uncertainty of 40 meV. The only cases where we found a slightly worse agreement were both systems obtained from Rh intercalation and the one obtained by intercalating Ru at the graphene/Ir(111) interface. All these systems were characterized by a higher disorder, indicating that these experimental systems were in part different from those simulated in the calculations. In particular, in the first two cases, the reason can be ascribed to the fact that a small portion of

Rh atoms were not completely intercalated but also formed clusters on the graphene surface, a behaviour previously observed for the low temperature Rh deposition on graphene/Ir(111) [41].

3.3. Discussion

From the comparison of the data obtained in the different intercalation experiments, it is clear that there are major differences in the geometric and electronic properties of the graphene layer among systems with a different chemical species at the interface. For example, the intercalation of Ir on graphene/Ru(0001) leads to a very weakly interacting graphene layer, as for graphene/Ir(111), while intercalation on graphene/Ir(111) leads to stronger interaction with the substrate, resulting in a buckling of the graphene layer. On the other hand, interfaces having the same chemical species show very similar properties regardless of the difference in the lattice parameter of the supporting substrate.

These results suggest that the key role in determining the strength of interaction is played by the chemical composition of the substrate. Geometry, on the other hand, mainly determines the periodicity of the moiré, which is preserved after intercalation. This is particularly obvious if we consider the case of graphene interacting with Co: it is flat and commensurate on Co(0001) [13], while it is buckled in the case of the Co intercalation.

A further proof of the important effects of the electronic structure and the composition of the substrate on its interaction with graphene comes from the correlation between the position of C atoms with respect to the surface sites and their C1s BE. As has been already mentioned, the BE — and therefore the interaction — is maximum for C atoms in on-top configuration and minimum for those in hollow sites, even among atoms located at the same distance from the substrate. This effect demonstrates that the interaction between graphene and metal surfaces depends on the hybridization

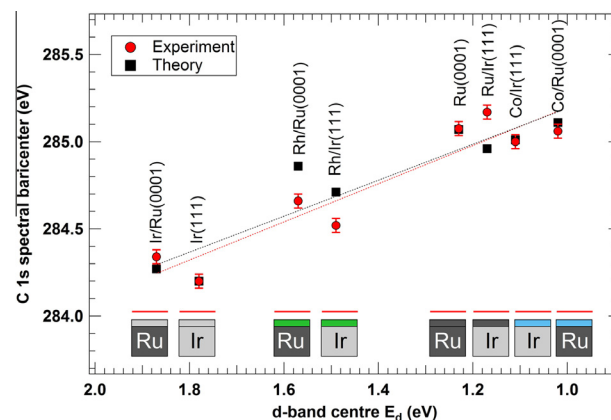


Fig. 8 – Theoretical (black squares) and experimental (red circles) values of the C1s core-level BE distribution's barycentre of all C atoms in the moiré unit cell, for each system studied in this work, versus the calculated d-band centre of the underlying clean metal surface. (A colour version of this figure can be viewed online.)

between the π_z orbitals of graphene and the d-band of the substrate [24].

In order to find the relationship between the C1s core levels and the chemical properties of the supporting substrates we plotted (in Fig. 8) the experimental and theoretical C1s spectral barycentres versus the calculated d-band centre of the topmost metallic layers. Indeed, as firstly pointed out by Wang et al. [17], and more recently extensively described by Toyoda et al. [25], d-band metals greatly influence the potential-energy surface of graphene on transition-metal surfaces and are largely responsible for the adsorption properties of graphene.

Besides the very good agreement between experimental (round markers) and theoretical (square markers) values, we found a strong linear relationship between C1s spectral centre of mass and calculated d-band centres. Although core-level BEs are certainly affected by final-state contributions which are intrinsic to the photoemission process, their contribution does not obscure this linear relationship. This offers a further proof that core level spectroscopy can be considered a useful experimental descriptor of the interaction strength of graphene with transition metal surfaces.

4. Conclusions

In summary, we have studied systems in which graphene is supported on monocrystalline transition metal surfaces constrained to the periodicity of Ir(111) and Ru(0001), both from a theoretical and experimental point of view. We have demonstrated that the chemical species of the topmost layer of the substrate plays a major role in determining the strength of interaction between graphene and its substrate. We have verified that the C1s spectral barycentre has a linear relationship with the d-band centre position, which is recognized to strongly influence the coupling between graphene and the metal surface. We have therefore demonstrated that C1s core level spectra contain relevant information on graphene–metal interfaces and can be considered a reliable descriptor of the graphene–substrate interaction strength.

Acknowledgements

We acknowledge the financial support from MIUR through the project PRIN entitled “GRAF. Frontiers in graphene research: understanding and controlling advanced functionalities” (N.20105ZZYSE001) and from the University of Trieste through the programme “Finanziamento di Ateneo per progetti di ricerca scientifica - FRA 2014”. N.J. acknowledges support from the International Centre for Theoretical Physics (ICTP) under the “Programme for Training and Research in Italian Laboratories” (TRIL). This work used the ARCHER UK National Supercomputing Service (<http://www.archer.ac.uk>).

Appendix A. Supplementary data

Supplementary data associated with this article can be found, in the online version, at <http://dx.doi.org/10.1016/j.carbon.2015.05.041>.

REFERENCES

- [1] Novoselov K, Geim A, Morozov S, Jiang D, Zhang Y, Dubonos S, et al. Electric field effect in atomically thin carbon films. *Science* 2004;306(5696):666–9. <http://dx.doi.org/10.1126/science.1102896>.
- [2] Novoselov KS, Geim AK, Morozov SV, Jiang D, Katsnelson MI, Grigorieva IV, et al. Two-dimensional gas of massless Dirac fermions in graphene. *Nature* 2005;438(7065):197–200. <http://dx.doi.org/10.1038/nature04233>.
- [3] Novoselov K, Fal'Ko V, Colombo L, Gellert P, Schwab M, Kim K. A roadmap for graphene. *Nature* 2012;490(7419):192–200. <http://dx.doi.org/10.1038/nature11458>.
- [4] Adamska L, Lin Y, Ross A, Batzill M, Oleynik I. Atomic and electronic structure of simple metal/graphene and complex metal/graphene/metal interfaces. *Phys Rev B* 2012;85(19):195443. <http://dx.doi.org/10.1103/PhysRevB.85.195443>.
- [5] Torre AL, Romdhane FB, Baaziz W, Janowska I, Pham-Huu C, Begin-Colin S, et al. Formation and characterization of carbon–metal nano-contacts. *Carbon* 2014;77(0):906–11. <http://dx.doi.org/10.1016/j.carbon.2014.06.004>.
- [6] Giovannetti G, Khomyakov P, Brocks G, Karpan V, Van Den Brink J, Kelly P. Doping graphene with metal contacts. *Phys Rev Lett* 2008;101(2):026803. <http://dx.doi.org/10.1103/PhysRevLett.101.026803>.
- [7] Varykhalov A, Scholz M, Kim T, Rader O. Effect of noble-metal contacts on doping and band gap of graphene. *Phys Rev B* 2010;82(12):121101. <http://dx.doi.org/10.1103/PhysRevB.82.121101>.
- [8] Schultz B, Jaye C, Lysaght P, Fischer D, Prendergast D, Banerjee S. On chemical bonding and electronic structure of graphene–metal contacts. *Chem Sci* 2013;4(1):494–502. <http://dx.doi.org/10.1039/c2sc21018e>.
- [9] Entani S, Kurahashi M, Sun X, Yamauchi Y. Spin polarization of single-layer graphene epitaxially grown on Ni(111) thin film. *Carbon* 2013;61(0):134–9. <http://dx.doi.org/10.1016/j.carbon.2013.04.077>.
- [10] Weser M, Voloshina E, Horn K, Dedkov Y. Electronic structure and magnetic properties of the graphene/Fe/Ni(111) intercalation-like system. *Phys Chem Chem Phys* 2011;13(16):7534–9. <http://dx.doi.org/10.1039/c1cp00014d>.
- [11] Abteu T, Shih B-C, Banerjee S, Zhang P. Graphene–ferromagnet interfaces: hybridization, magnetization and charge transfer. *Nanoscale* 2013;5(5):1902–9. <http://dx.doi.org/10.1039/c2nr32972g>.
- [12] Preobrajenski A, Ng M, Vinogradov A, Mårtensson N. Controlling graphene corrugation on lattice-mismatched substrates. *Phys Rev B* 2008;78(7):073401. <http://dx.doi.org/10.1103/PhysRevB.78.073401>.
- [13] Batzill M. The Surf. Sci. of graphene: metal interfaces, CVD synthesis, nanoribbons, chemical modifications, and defects. *Surf Sci Rep* 2012;67(3-4):83–115. <http://dx.doi.org/10.1016/j.surfrep.2011.12.001>.
- [14] Busse C, Lazić P, Djemour R, Coraux J, Gerber T, Atodiresei N, et al. Graphene on Ir(111): physisorption with chemical modulation. *Phys Rev Lett* 2011;107(3):036101. <http://dx.doi.org/10.1103/PhysRevLett.107.036101>.
- [15] Sutter P, Sadowski J, Sutter E. Graphene on Pt(111): growth and substrate interaction. *Phys Rev B* 2009;80(24):245411. <http://dx.doi.org/10.1103/PhysRevB.80.245411>.
- [16] Marchini S, Günther S, Wintterlin J. Scanning tunneling microscopy of graphene on Ru(0001). *Phys Rev B* 2007;76(7):075429. <http://dx.doi.org/10.1103/PhysRevB.76.075429>.
- [17] Wang B, Bocquet M-L, Marchini S, Günther S, Wintterlin J. Chemical origin of a graphene moiré overlayer on Ru(0001).

- Phys Chem Chem Phys 2008;10(24):3530–4. <http://dx.doi.org/10.1039/b801785a>.
- [18] Alfè D, Pozzo M, Miniussi E, Günther S, Lacovig P, Lizzit S, et al. Fine tuning of graphene–metal adhesion by surface alloying. *Sci Rep* 2013;3:2430. <http://dx.doi.org/10.1038/srep02430>.
- [19] Miniussi E, Pozzo M, Baraldi A, Vesselli E, Zhan R, Comelli G, et al. Thermal stability of corrugated epitaxial graphene grown on Re(0001). *Phys Rev Lett* 2011;106(21):216101. <http://dx.doi.org/10.1103/PhysRevLett.106.216101>.
- [20] Miniussi E, Pozzo M, Menteş T, Niño M, Locatelli A, Vesselli E, et al. The competition for graphene formation on Re (0001): a complex interplay between carbon segregation, dissolution and carburisation. *Carbon* 2014;73:389–402. <http://dx.doi.org/10.1016/j.carbon.2014.02.081>.
- [21] Wintterlin J, Bocquet M-L. Graphene on metal surfaces. *Surf Sci* 2009;603(10–12):1841–52. <http://dx.doi.org/10.1016/j.susc.2008.08.037>.
- [22] Merino P, Švec M, Pinardi AL, Otero G, Martín-Gago JA. Strain-driven Moiré superstructures of epitaxial graphene on transition metal surfaces. *ACS Nano* 2011;5(7):5627–34. <http://dx.doi.org/10.1021/nn201200j>.
- [23] Frank O, Vejpravova J, Holy V, Kavan L, Kalbac M. Interaction between graphene and copper substrate: the role of lattice orientation. *Carbon* 2014;68(0):440–51. <http://dx.doi.org/10.1016/j.carbon.2013.11.020>.
- [24] Hammer B, Nørskov J. Theoretical Surf. Sci. and catalysis-calculations and concepts. *Adv Cat* 2000;45:71–129. [http://dx.doi.org/10.1016/S0360-0564\(02\)45013-4](http://dx.doi.org/10.1016/S0360-0564(02)45013-4).
- [25] Toyoda K, Nozawa K, Matsukawa N, Yoshii S. Density functional theoretical study of graphene on transition-metal surfaces: the role of metal d-band in the potential-energy surface. *J Phys Chem C* 2013;117(16):8156–60. <http://dx.doi.org/10.1021/jp311741h>.
- [26] Das S, Lahiri D, Lee D-Y, Agarwal A, Choi W. Measurements of the adhesion energy of graphene to metallic substrates. *Carbon* 2013;59(0):121–9. <http://dx.doi.org/10.1016/j.carbon.2013.02.063>.
- [27] Schultz B, Dennis R, Lee V, Banerjee S. An electronic structure perspective of graphene interfaces. *Nanoscale* 2014;6(7):3444–66. <http://dx.doi.org/10.1039/c3nr06923k>.
- [28] Kralj M, Pletikosić I, Petrović M, Pervan P, Milun M, N'Diaye A, et al. Graphene on Ir(111) characterized by angle-resolved photoemission. *Phys Rev B* 2011;84(7):075427. <http://dx.doi.org/10.1103/PhysRevB.84.075427>.
- [29] Varykhalov A, Sánchez-Barriga J, Shikin A, Biswas C, Vescovo E, Rybkin A, et al. Electronic and magnetic properties of quasifreestanding graphene on Ni. *Phys Rev Lett* 2008;101(15):157601. <http://dx.doi.org/10.1103/PhysRevLett.101.157601>.
- [30] Brugger T, Günther S, Wang B, Dil J, Bocquet M-L, Osterwalder J, et al. Comparison of electronic structure and template function of single-layer graphene and a hexagonal boron nitride nanomesh on Ru(0001). *Phys Rev B* 2009;79(4):045407. <http://dx.doi.org/10.1103/PhysRevB.79.045407>.
- [31] Pletikosić I, Kralj M, Pervan P, Brako R, Coraux J, N'Diaye A, et al. Dirac cones and minigaps for graphene on Ir(111). *Phys Rev Lett* 2009;102(5):056808. <http://dx.doi.org/10.1103/PhysRevLett.102.056808>.
- [32] Varykhalov A, Rader O. Graphene grown on Co(0001) films and islands: electronic structure and its precise magnetization dependence. *Phys Rev B* 2009;80(3):035437. <http://dx.doi.org/10.1103/PhysRevB.80.035437>.
- [33] Enderlein C, Kim Y, Bostwick A, Rotenberg E, Horn K. The formation of an energy gap in graphene on ruthenium by controlling the interface. *NJ Phys* 2010;12:033014. <http://dx.doi.org/10.1088/1367-2630/12/3/033014>.
- [34] Generalov A, Dedkov Y. EELS study of the epitaxial graphene/Ni(111) and graphene/Au/Ni(111) systems. *Carbon* 2012;50(1):183–91. <http://dx.doi.org/10.1016/j.carbon.2011.08.018>.
- [35] Lizzit S, Zampieri G, Petaccia L, Larciprete R, Lacovig P, Rienks E, et al. Band dispersion in the deep 1s core level of graphene. *Nat Phys* 2010;6(5):345–9. <http://dx.doi.org/10.1038/nphys1615>.
- [36] Dahal A, Addou R, Coy-Diaz H, Lallo J, Batzill M. Charge doping of graphene in metal/graphene/dielectric sandwich structures evaluated by C-1s core level photoemission spectroscopy. *APL Mater* 2013;1(4):042107. <http://dx.doi.org/10.1063/1.4824038>.
- [37] Abrami A, Barnaba M, Battistello L, Bianco A, Brena B, Cautero G, et al. Super ESCA: first beamline operating at ELETTRA. *Rev Sci Instrum* 1995;66(2):1618–20. <http://dx.doi.org/10.1063/1.1145862>.
- [38] N'Diaye A, Coraux J, Plasa T, Busse C, Michely T. Structure of epitaxial graphene on Ir(111). *NJ Phys* 2008;10:043033. <http://dx.doi.org/10.1088/1367-2630/10/4/043033>.
- [39] Lizzit S, Baraldi A. High-resolution fast X-ray photoelectron spectroscopy study of ethylene interaction with Ir(111): from chemisorption to dissociation and graphene formation. *Catal Today* 2010;154(1–2):68–74. <http://dx.doi.org/10.1016/j.cattod.2010.05.028>.
- [40] Vo-Van C, Schumacher S, Coraux J, Sessi V, Fruchart O, Brookes N, et al. Magnetism of cobalt nanoclusters on graphene on iridium. *Appl Phys Lett* 2011;99(14):142504. <http://dx.doi.org/10.1063/1.3646480>.
- [41] Cavallin A, Pozzo M, Africh C, Baraldi A, Vesselli E, Dri C, et al. Local electronic structure and density of edge and facet atoms at Rh nanoclusters self-assembled on a graphene template. *ACS Nano* 2012;6(4):3034–43. <http://dx.doi.org/10.1021/nn300651s>.
- [42] Zhou Z, Habenicht B, Guo Q, Yan Z, Xu Y, Liu L, et al. Graphene moiré structure grown on a pseudomorphic metal overlayer supported on Ru(0001). *Surf Sci* 2013;611:67–73. <http://dx.doi.org/10.1016/j.susc.2013.01.016>.
- [43] Vlačić S, Kimouche A, Coraux J, Santos B, Locatelli A, Rougemaille N. Cobalt intercalation at the graphene/iridium(111) interface: influence of rotational domains, wrinkles, and atomic steps. *Appl Phys Lett* 2014;104(10):101602. <http://dx.doi.org/10.1063/1.4868119>.
- [44] Doniach S, Sunjic M. Many-electron singularity in X-ray photoemission and X-ray line spectra from metals. *J Phys C* 1970;3(2):285–91. <http://dx.doi.org/10.1088/0022-3719/3/2/010>.
- [45] Shirley D. High-resolution X-ray photoemission spectrum of the valence bands of gold. *Phys Rev B* 1972;5(12):4709–14. <http://dx.doi.org/10.1103/PhysRevB.5.4709>.
- [46] Végh J. The analytical form of the Shirley-type background. *J Electron Spectrosc Relat Phenom* 1988;46(2):411–7. [http://dx.doi.org/10.1016/0368-2048\(88\)85038-2](http://dx.doi.org/10.1016/0368-2048(88)85038-2).
- [47] Hohenberg P, Kohn W. Inhomogeneous electron gas. *Phys Rev* 1964;136(3B):B864–71. <http://dx.doi.org/10.1103/PhysRev.136.B864>.
- [48] Kohn W, Sham LJ. Self-consistent equations including exchange and correlation effects. *Phys Rev* 1965;140(4A):A1133–8. <http://dx.doi.org/10.1103/PhysRev.140.A1133>.
- [49] Perdew JP, Burke K, Ernzerhof M. Generalized gradient approximation made simple. *Phys Rev Lett* 1996;77:3865–8. <http://dx.doi.org/10.1103/PhysRevLett.77.3865>.
- [50] Blöchl PE. Projector augmented-wave method. *Phys Rev B* 1994;50(24):17953–79. <http://dx.doi.org/10.1103/PhysRevB.50.17953>.
- [51] Kresse G, Furthmüller J. Efficient iterative schemes for ab initio total-energy calculations using a plane-wave basis

- set. Phys Rev B 1996;54(16):11169–86. <http://dx.doi.org/10.1103/PhysRevB.54.11169>.
- [52] Kresse G, Joubert D. From ultrasoft pseudopotentials to the projector augmented-wave method. Phys Rev B 1999;59(3):1758–75. <http://dx.doi.org/10.1103/PhysRevB.59.1758>.
- [53] Köhler L, Kresse G. Density functional study of CO on Rh(111). Phys Rev B 2004;70:165405. <http://dx.doi.org/10.1103/PhysRevB.70.165405>.
- [54] Lizzit S, Larciprete R, Lacovig P, Dalmiglio M, Orlando F, Baraldi A, et al. Transfer-free electrical insulation of epitaxial graphene from its metal substrate. Nano Lett 2012;12(9):4503–7. <http://dx.doi.org/10.1021/nl301614j>.
- [55] Lacovig P, Pozzo M, Alfè D, Vilmercati P, Baraldi A, Lizzit S. Growth of dome-shaped carbon nanoislands on Ir(111): the intermediate between carbidic clusters and quasi-free-standing graphene. Phys Rev Lett 2009;103(16):166101. <http://dx.doi.org/10.1103/PhysRevLett.103.166101>.
- [56] Casarin B, Cian A, Feng Z, Monachino E, Randi F, Zamborlini G, et al. The thinnest carpet on the smallest staircase: the growth of graphene on Rh(533). J Phys Chem C 2014;118(12):6242–50. <http://dx.doi.org/10.1021/jp411582a>.
- [57] Gotterbarm K, Zhao W, Höfert O, Gleichweit C, Papp C, Steinrück H-P. Growth and oxidation of graphene on Rh(111). Phys Chem Chem Phys 2013;15(45):19625–31. <http://dx.doi.org/10.1039/c3cp53802h>.
- [58] Gotterbarm K, Steiner C, Bronnbauer C, Bauer U, Steinrück H-P, Maier S, et al. Graphene-templated growth of Pd nanoclusters. J Phys Chem C 2014;118(29):15934–9. <http://dx.doi.org/10.1021/jp5052563>.
- [59] Moritz W, Wang B, Bocquet M-L, Brugger T, Greber T, Wintterlin J, et al. Structure determination of the coincidence phase of graphene on Ru(0001). Phys Rev Lett 2010;104(13):136102. <http://dx.doi.org/10.1103/PhysRevLett.104.136102>.
- [60] Pacilé D, Lisi S, Di Bernardo I, Papagno M, Ferrari L, Pisarra M, et al. Electronic structure of graphene/Co interfaces. Phys Rev B 2014;90(19):195446. <http://dx.doi.org/10.1103/PhysRevB.90.195446>.
- [61] Eom D, Prezzi D, Rim K, Zhou H, Lefenfeld M, Xiao S, et al. Structure and electronic properties of graphene nanoislands on CO(0001). Nano Lett 2009;9(8):2844–8. <http://dx.doi.org/10.1021/nl900927f>.
- [62] Voloshina E, Dedkov Y. Graphene on metallic surfaces: problems and perspectives. Phys Chem Chem Phys 2012;14(39):13502–14. <http://dx.doi.org/10.1039/c2cp42171b>.
- [63] Hamada I, Otani M. Comparative van der Waals density-functional study of graphene on metal surfaces. Phys Rev B 2010;82(15):153412. <http://dx.doi.org/10.1103/PhysRevB.82.153412>.
- [64] Wang B, Caffio M, Bromley C, Früchtl H, Schaub R. Coupling epitaxy, chemical bonding, and work function at the local scale in transition metal-supported graphene. ACS Nano 2010;4(10):5773–82. <http://dx.doi.org/10.1021/nn101520k>.